Chemistry & Biology
Brief Communication

Halogen Bonds Form the Basis for Selective P-TEFb Inhibition by DRB

Sonja Baumli,[1,*] Jane A. Endicott,[1] and Louise N. Johnson[1]
[1]Department of Biochemistry/Laboratory of Molecular Biophysics, University of Oxford, Oxford, OX1 3QU, UK
*Correspondence: Sonja.baumli@bioch.ox.ac.uk
DOI 10.1016/j.chembiol.2010.07.012

SUMMARY

Cdk9, the kinase of the positive transcription elongation factor b, is required for processive transcription elongation by RNA polymerase II. Cdk9 inhibition contributes to the anticancer activity of many Cdk inhibitors under clinical investigation and hence there is interest in selective Cdk9 inhibitors. DRB (5,6-dichlorobenzimidazone-1-β-D-ribofuranoside) is a commonly used reagent for Cdk9 inhibition in cell biology studies. The crystal structures of Cdk9 and Cdk2 in complex with DRB reported here describe the molecular basis for the DRB selectivity toward Cdk9. The DRB chlorine atoms form halogen bonds that are specific for the Cdk9 kinase hinge region. Kinetic and thermodynamic experiments validate the structural findings and implicate the C-terminal residues of Cdk9 in contributing to the affinity for DRB. These results open the possibility to exploit halogen atoms in inhibitor design to specifically target Cdk9.

INTRODUCTION

The positive transcription elongation factor b (P-TEFb; Cdk9/Cyclin T [CycT]) stimulates transcription elongation by RNA polymerase II (Pol II). After initiation of transcription by Pol II, transcription is halted by the repressors 5,6-dichlorobenzimidazone-1-β-D-ribofuranoside (DRB)-sensitivity-inducing factor (DSIF) and the negative elongation factor (NELF). In the presence of these repressors Pol II produces short mRNA transcripts and pauses. Cdk9 as a subunit of P-TEFb is recruited to the halted transcription complex and phosphorylates DSIF, NELF and the Pol II C-terminal domain (CTD) (Core and Lis, 2008; Peterlin and Price, 2006; Yamada et al., 2006). These phosphorylations relieve repressor activity and are accompanied by recruitment of mRNA processing enzymes and the loss of NELF that together allow transcription to progress to the elongation phase.

DRB has been established as an inhibitor of mRNA synthesis (Sehgal et al., 1976) and is a widely used agent that specifically inhibits transcription elongation, but not initiation. DRB inhibits P-TEFb with a IC_{50} of 0.9–0.34 μM (Peng et al., 1998; Wang and Fischer, 2008). DRB is selective for Cdk9 and the IC_{50} value is two orders of magnitude less than the action of DRB toward other Cdks (Cdk1/CycB:IC_{50} ~17 μM [Wang and Fischer, 2008]).

P-TEFb is a validated drug target in oncology, virology, and cardiology (Wang and Fischer, 2008). It is most relevant as a target when the diseased state has arisen from the upregulation of proteins that have unstable mRNA (Lam et al., 2001). Flavopiridol, a potent P-TEFb inhibitor (K_i ~3 nM) has advanced to Phase II clinical trials for the treatment of chronic lymphocytic leukemia (Byrd et al., 2007). Although DRB is not a drug candidate, understanding its mode of P-TEFb inhibition is relevant for the study of transcription regulation and may allow the design of more specific inhibitors to exploit the clinical potential of P-TEFb inhibition.

Protein kinase structural studies have shown that adenosine triphosphate (ATP) binds with the adenine moiety docked into a hydrophobic cleft between the two lobes of the kinase domain, interacting with the kinase hinge region through hydrogen bonds (Figure 1). Many kinase inhibitors bind at this highly conserved nucleotide binding site. For example, flavopiridol makes ATP-like hydrogen bond interactions (Baumli et al., 2008). DRB is an adenosine analog and hence it might be expected to bind to the ATP binding site (Figure 1). However, in DRB the hydrogen bonding groups are replaced by chlorine. It is not clear how DRB might bind to P-TEFb and nor is it understood how DRB achieves specificity for Cdk9 compared with other Cdks.

To answer these questions, we have determined the crystal structures of Cdk9/CycT and Cdk2/CycA in complex with DRB. Bound to Cdk9, DRB interacts via its chlorine atoms forming halogen bonds to the main chain carbonyl oxygens from the hinge region whereas the adenine-like moiety and ribose are accommodated in similar regions to those occupied by ATP. DRB binds to Cdk2 in an alternative conformation that exploits only one halogen bond and a halogen/π electron interaction. It is proposed that the inherent flexibility of Cdk9 in complex with CycT compared to the more rigid conformation of Cdk2 in complex with CycA contributes to specificity and affinity.

RESULTS

The DRB Binding Site in Cdk9/CycT and Cdk2/CycA

The structures of active phospho-$Cdk9_{330}$ (residues 1–330)/CycT (residues 1–259) and phospho-Cdk2/CycA (residues 175–432) in complex with DRB were solved at 2.8 Å and 2.1 Å resolution, respectively (Table 1). In both Cdk/Cyclin complexes DRB binds to the ATP binding site adopting different, kinase-specific, orientations.

In Cdk9/CycT, the planar benzimidazole moiety locates to the adenine binding site and is sandwiched between Ile25 in

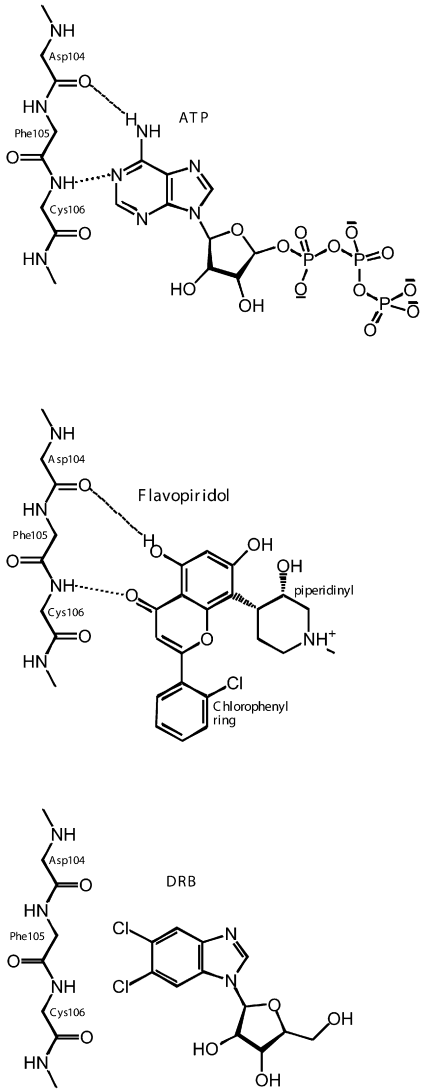

Figure 1. The Chemical Structures of Adenosine Triphosphate, Flavopiridol, and 5,6-Dichlorobenzimidazone-1-β-D-Ribofuranoside Drawn Bound to a Schematic Representation of the Cdk9 Hinge Region

Table 1. Data Collection and Refinement Statistics

	Cdk9/CycT/DRB	Cdk2/CycA/DRB
Data collection		
Beam line	ESRF ID23-1	ESRF ID14-4
Space group and unit cell (Å)	H3	$P2_12_12_1$
	a = b = 173.8, c = 99.2	a = 74.3, b = 132.3, c = 148.4
Resolution (Å) (highest resolution shell)	38.5–2.8 (2.95–2.80)	59.5–2.1 (2.21–2.10)
Total observations	153,549 (22,767)	352,234 (51,715)
Unique	27,472 (3998)	87,151 (12,597)
R_{merge}	0.066 (0.597)	0.098 (0.595)
Multiplicity	5.6 (5.7)	4.0 (4.1)
Mean I/σI	18.6 (2.2)	10.2 (2.6)
Completeness %	99.9 (100)	99.9 (100)
Refinement		
Total number of atoms	4701	9419
Number of waters	28	525
R (highest resolution shell)	17.5 (29.3 [2.85–2.8])	18.0 (26.6 [2.12–2.1])
R_{free} (highest resolution shell)	21.4 (32.6 [2.85–2.8])	21.9 (29.9 [2.12–2.1])
Rmsd bonds (Å)	0.008	0.007
Rmsd angles (°)	1.2	1.1

Rmsd: root-mean-square-deviation.

the N-terminal lobe and Leu156 in the C-terminal lobe of Cdk9 (Figure 2A). The two chlorine atoms of the DRB benzimidazole moiety contact the hinge region: there are contacts from DRB Cl1 to the main chain oxygen of Asp104 (distance: 2.7 Å; angles: C = O—Cl1 129°; C-Cl1—O 174°) and from DRB Cl2 to the main chain oxygen of Cys106 (3.0 Å; angles: C = O—Cl2 127°; C-Cl2—O 160°) (Figure 2C). These contacts are consistent with geometries reported for halogen bonds, defined as interactions where the approach of the halogen to an electronegative atom is closer than the sum of their van der Waals (vdW) radii (Auffinger et al., 2004). For a chlorine (vdW radius 1.75 Å) and oxygen (vdW radius 1.52 Å) the distance is 3.27 Å. In addition there is a contact from Cl2 to NH Cys106 (3.5 Å; angle Cl2—N-H = 148°) consistent with a contact in which the halogen acts as a hydrogen bond acceptor (Lu et al., 2009b). The only other polar contact observed between DRB and Cdk9 is a water-mediated interaction between the benzimidazole N2 and the backbone NH group of Asp167. The halogen bonds appear to be the major determining factor for the specific orientation of DRB bound to Cdk9.

In Cdk2/CycA, DRB also binds to the ATP site but in a different orientation (Figures 2B and 2D). Cl1 contacts the backbone carbonyl of the hinge-region Glu81 (distance: 2.7Å; angles: C = O—Cl1 153°; C-Cl1—O 166°) making one contact that is similar to a contact observed in Cdk9. Cl2 points toward the gatekeeper residue Phe80 at the back of the Cdk2 ATP binding site such that the halogen contacts the π-electrons of the phenylalanine ring (angle 70°; distance to plane of ring: 4.0 Å). The ribofuranoside adopts a similar orientation in the Cdk2 bound structure as in Cdk9 but it is less ordered. This orientation is achieved by a rotation of 121° around the C1-N1 bond that connects the ribofuranoside to the benzimidazole moiety. There is a direct hydrogen bond from the ribofuranoside to the main chain nitrogen of Gly13. There are also several water-bridged interactions of DRB with Cdk2. These include water bridges between N2 in the benzimidazole moiety and the backbone carbonyls of Leu83 and His84, and the ribofuranoside to Asp86 and to Asn132 (Figure 2B). The higher resolution of the Cdk2 structure (2.1 Å) compared with that for Cdk9 (2.8 Å) permitted a greater number of water molecules to be built with confidence into the structure.

Refinement of the occupancy of DRB in the Cdk2 bound structure suggested that ~12% of the DRB molecules bind in a Cdk9-like orientation. Thus it is possible for DRB to adopt a Cdk9 binding mode also in Cdk2, but this is not the preferred orientation. Residues 107–109 in the hinge region of Cdk9 adopt

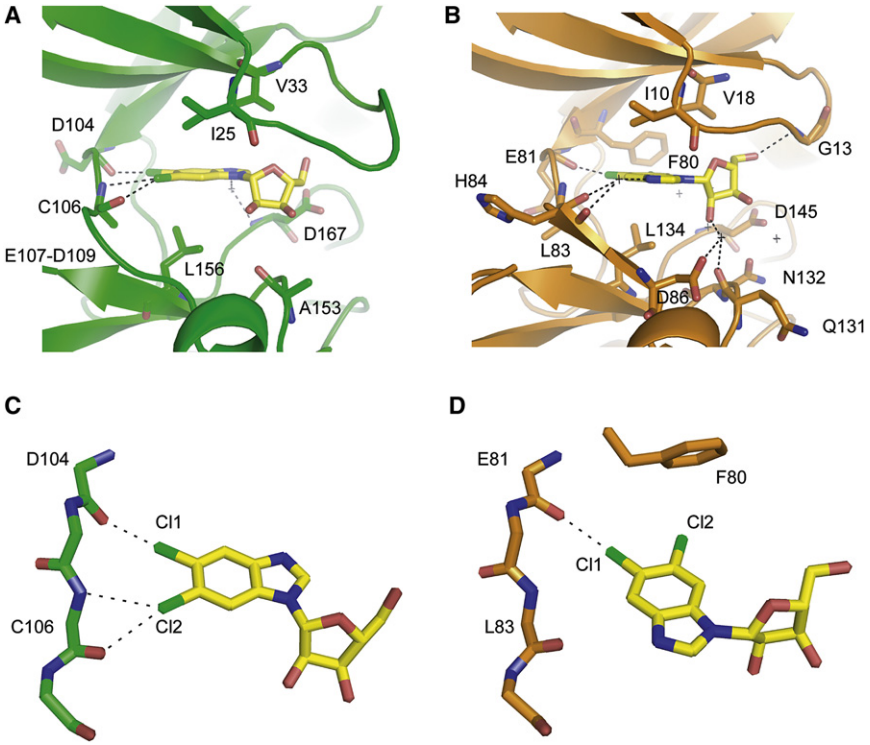

Figure 2. DRB Binding to Cdk9 and Cdk2

(A) Details of the Cdk9/CycT ATP binding site complexed with DRB.

(B) Details of the Cdk2/CycA ATP binding site complexed with DRB. Inhibitor carbon atoms are colored yellow and contacting residues are drawn as stick models. Halogen and hydrogen bonds are indicated by dotted lines. Waters are shown as crosses.

(C and D) Detailed views of the halogen bonds of DRB bound to Cdk9 and Cdk2, respectively.

a different path to that of the corresponding residues in Cdk2 so that the carbonyl of Cys106 is displaced backward by 0.8 Å with respect to the corresponding residue in Cdk2 (Leu83). This small change in position allows more space to optimally accommodate DRB Cl2 and form the halogen bonds to the Cdk9 hinge region. Thus it seems that the halogen bond formation requires a very specific environment and is therefore a determinant of selectivity.

DRB Binding Induces Conformational Changes in Cdk9 but Not Cdk2

Cdk9 is less constrained by contacts to CycT than Cdk2 bound to CycA and is therefore inherently more flexible (Baumli et al., 2008). On DRB binding to Cdk9/CycT, the two kinase lobes rotate around the Phe105-Cys106 peptide bond in the hinge region by ~8° and move toward each other to accommodate the inhibitor in the ATP binding site (Figure 3A). The major structural changes in Cdk9 are in the glycine-rich loop, which moves downward to enclose the inhibitor. Concomitantly, the β3-αC loop folds over the glycine-rich loop and locks it in its downward position (gray to blue in Figure 3A). Leu51 fills the hydrophobic pocket previously occupied by Phe30 of the glycine-rich loop. These changes are specific to Cdk9 and do not occur in the Cdk2/CycA bound structure (gray to orange in Figure 3B). All other Cdks have a charged residue at the position equivalent to Leu51 in Cdk9 (e.g., Arg36 in Cdk2). These residues are unable to fill the vacant hydrophobic pocket created by the shift of the glycine-rich loop.

Although DRB makes more polar contacts with Cdk2 than it does when bound to Cdk9, DRB bound to Cdk9/CycT is able to exploit the greater flexibility of the kinase to increase favorable van der Waals contacts. The downward conformations of the glycine-rich loop and the β3-αC loop are reminiscent of those observed on flavopiridol binding to Cdk9 and may account for the increased potency toward Cdk9 for both inhibitors.

The Cdk9 C Terminus Contributes to the Inhibitor Affinity

To validate our structural results, we measured the ability of DRB to inhibit the crystallized variants of the Cdk/Cyclin complexes. The measured IC_{50} values are 3.6 μM for the C-terminally truncated Cdk9 (residues 1–330)/CycT, 0.23 μM for the full-length Cdk9 (residues 1–372)/CycT, and 65 μM for Cdk2/CycA (Table 2; see Figure S1A available online). The apparent increase in effectiveness of DRB as an inhibitor of Cdk9/CycT compared with Cdk2/CycA is consistent with the structural results. The IC_{50} value (0.23 μM) for $Cdk9_{FL}$/CycT is consistent with published results (IC_{50} values between 0.9 and 0.34 μM [Peng et al., 1998; Wang and Fischer, 2008]) and because this value is lower than that for the truncated $Cdk9_{330}$, it suggests that the C-terminal portion of the full-length Cdk9 influences the inhibition by DRB. Examination of the structure of Cdk9/CycT suggests that the C-terminal residues could wrap around the catalytic site further shielding the inhibitor from solvent (Figure 3A) and stabilize the adopted kinase conformation. Indeed, when we test the stability of the Cdk9/CycT/DRB variants in thermal denaturation assays $Cdk9_{FL}$/CycT shows a small increase (49.26 ± 0.05°C) in its melting point compared with $Cdk9_{330}$/CycT (48.76 ± 0.07°C). This stabilization is specific to DRB and does not occur in the other Cdk9/inhibitor complexes tested (Figure S1B) suggesting that the C-terminal residues contribute to the overall stability of the DRB complexes.

DISCUSSION

The binding of DRB to Cdk9/CycT is mostly directed by halogen bonds. These interactions are analogous to hydrogen bonds with the halogen acting as the electron acceptor and the oxygen acting as the electron donor. Many examples of halogen bonds have been identified in the Cambridge Crystallographic Database for small molecule compounds (Lommerse et al.,

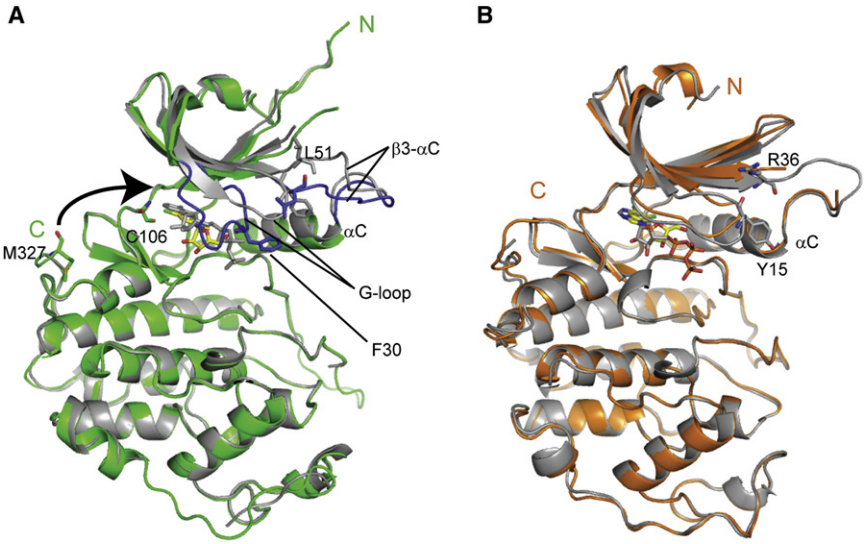

Figure 3. DRB Binding Is Accompanied by Conformational Change

(A) Cdk9/CycT/DRB (green) and Cdk9/CycT/ATP (gray; 3BLQ) are superimposed on their C-terminal lobes. Conformational changes occur in the glycine-rich loop, the β3-αC loop (blue) and in a rotation of the Cdk9 N-terminal kinase domain around Cys106 in the hinge region. The C-terminal residue Met327 is marked and the arrow indicates the possible direction of C-terminal residues 331–372.

(B) Cdk2/CycA/DRB (orange) and Cdk2/CycA/ATP (gray; 1QMZ) have been superposed as in (A). The Cyclin subunits are omitted. There are breaks in the electron density in Cdk9 between residues 88–96 (β4-β5 loop) and in Cdk2 between residues 37–41 (β3-αC loop).

1996). 248 O—X interactions have been described in the PDB demonstrating that they also have roles in macromolecular assemblies (Lu et al., 2009a). A systematic analysis by Auffinger et al. (2004) identified over 100 short halogen contacts in the PDB, of which ~70% were C = O—X, where X is Cl, Br, or I. These had a preferred geometry with angles C = O—X ~120° and C-X—O ~165° or 145°.

Ab initio electrostatic potential calculations show that the halogen develops an electropositive crown along the C-X axis, which is surrounded by a neutral region and then by an electronegative belt (Auffinger et al., 2004). The magnitude of the effect increases such that I > Br > Cl and is modulated by the chemical context of the halogen atom. There are larger effects for halogens associated with electron withdrawing groups so that, for example, the effects are more pronounced for halogens in aromatic than aliphatic compounds (Auffinger et al., 2004). This charge distribution allows both, electrophile "head-on" and nucleophile "side-on" interactions with halogens. In the Cdk9/DRB complex both types of interactions are exploited: the carbonyl oxygens are directed toward the positive crown of the chlorines in head on interactions and these contacts are augmented by a side on interaction in which the N-H is directed toward the halogen electronegative belt.

A specific chemical environment is required for halogen bonds to be formed. This is demonstrated by the current results where DRB binds in alternative ways to Cdk9/CycT and to Cdk2/CycA. The only other structural result with DRB bound to a kinase is with CK2 where DRB makes lower affinity interactions at the ATP binding site and at a second allosteric site (K_i competitive: 29 μM, K_i noncompetitive: 39.7 μM [Raaf et al., 2008]). The inhibitor binding mode at the ATP site is different from both the Cdk9 and Cdk2 interactions and DRB forms a weak halogen bond to the CK2 hinge region. Halogen bond formation contributes to the specific molecular recognition in DRB/Cdk9 interactions. However, halogen bonds are weak interactions. The binding energy of a halogen bond has been estimated to range from about half to slightly more than that of a hydrogen bond, depending on the geometry of the binding site. The formation of the halogen bonds cannot account for the potency of DRB toward Cdk9. Rather, vdW contacts and stabilization of a favorable kinase conformation also contribute to the higher affinity of the inhibitor toward Cdk9 compared with Cdk2. This effect is further increased by the C-terminal kinase residues that stabilize the adopted conformation.

Table 2. Cdk9 and Cdk2 Inhibition by DRB and Melting Temperature of CDK9

Kinase	IC_{50} (μM)	T_m (°C)
$Cdk9_{FL}$/CycT	0.24	49.26 ± 0.05
$CDK9_{330}$/CycT	3.58	48.76 ± 0.07
Cdk2/CycA	65	ND

DRB: 5,6-dichlorobenzimidazone-1-β-D-ribofuranoside; ND: not determined. Errors are given as maximal deviations. Primary data are available in Figure S1.

A diversity of binding modes has been observed with the CK2 inhibitor 4,5,6,7-tetrabromobenzotriazole (TBB) and its derivatives. TBB binds to CK2 without forming halogen bonds to the kinase hinge region (Battistutta et al., 2005). Modifications of TBB that remove the negative charge of its triazole ring did generate compounds that bind to CK2 utilizing halogen bonds to the main chain carbonyl oxygens in the hinge region. All TBB derivatives are of similar potency toward CK2 ranging from IC_{50} of 0.14 μM to 0.74 μM, and slightly higher affinity does not correlate with the formation of halogen bonds (Battistutta et al., 2005). TBB also binds to the Cdk2/CycA ATP binding site but with a much lower affinity (IC_{50} = 16 μM [De Moliner et al., 2003]). In complex with Cdk2 TBB exploits the halogen-π interaction observed in the Cdk2-DRB structure and forms halogen bonds to the main chain carbonyl oxygens in the hinge region, adopting the binding mode of the TBB derivatives bound to CK2. Similar to the Cdk9 DRB interaction the potency of TBB and derivatives toward CK2 has been attributed to the induced conformational changes and burying of the inhibitor.

Taken together it is apparent that halogen bonds can confer selectivity toward a given kinase because they determine the

orientation in which the inhibitor is bound. However, additional contributions are needed to increase the potency of the compounds. Our structural studies can serve as the basis to improve the inhibitory potency of DRB without losing its specificity for Cdk9.

SIGNIFICANCE

5,6-dichlorobenzimidazone-1-β-D-ribofuranoside (DRB) is a widely used inhibitor of transcription elongation, which acts by specifically inhibiting P-TEFb, the positive transcription elongation factor b (Cdk9/CycT). We describe the binding mode of DRB to a C-terminally truncated Cdk9/CycT. DRB binds to the ATP binding site via halogen bonds from the chlorine to the main chain carbonyl oxygen atoms in the hinge region that connects the N- and C-terminal kinase lobes. Halogen bond formation determines the orientation of DRB within the ATP binding site. In addition, inhibitor binding induces conformational changes in the glycine-rich loop and the β3-αC loop that enclose the inhibitor. These interactions contribute to a high affinity interaction that is further enhanced by the Cdk9 C-terminal residues 331–372. In contrast, DRB binding to Cdk2/CycA is 282-fold weaker. The more restricted ATP site results in DRB binding in a different orientation to Cdk2/CycA. The structural studies indicate that halogen bonds contribute to binding and specificity and may be exploited to develop inhibitors that specifically target Cdk9.

EXPERIMENTAL PROCEDURES

Cdk9 (residues 1–330)/CycT1 (residues 1–259) was crystallized as described (Baumli et al., 2008). Crystals were soaked in the mother liquor containing 15% glycerol and 250 μM DRB for 30 min before cryo-cooling in liquid nitrogen. Cdk2 (residues 1–298)/CycA (residues 174–432) was prepared as described (Brown et al., 1999) and incubated with 2.6 mM DRB for 30 min. Insoluble DRB was removed by filtration (Amicon) before crystallization. Co-crystals were grown in 1.1 M $(NH_4)_2SO_4$, 100 mM HEPES pH 7.0, 5 mM dithiothreitol (DTT), cryo-protected in 7 M sodium formate containing DRB.

Data were processed using MOSFLM and programs from CCP4 (1994). Structures were solved with PHASER (McCoy et al., 2007) and improved by alternative rebuilding in COOT (Emsley and Cowtan, 2004) and refinement with PHENIX.REFINE (Afonine et al., 2005).

Kinase assays were carried out using a GST fusion of the Pol II CTD as a substrate for both kinases. Ten microliter reactions containing 15 μg GST-CTD, 12.5 ng of the respective Cdk/Cyclin complex in 10 μM ATP, 10 mM $MgCl_2$, 50 mM Tris/HCl pH 8.0, 0.2 μCi γ-^{32}P-labeled ATP were incubated for 5 min at 30°C and the reaction terminated by the addition of sodium dodecyl sulfate sample buffer. Samples were analyzed by sodium dodecyl sulfate polyacrylamide gel electrophoresis and autoradiography. Data were fitted with GraphPad Prism version 5.02 (www.graphpad.com).

Melting curves were determined using 1 μM of the respective Cdk/Cyclin complex with 1:1000 dilution of Sypro Orange (Molecular Probes) and 33 μM of the corresponding inhibitor in 20 mM HEPES pH 7.5, 500 mM NaCl, 10% glycerol, and 5 mM DTT. Spectra were obtained on a Stratagene mx3005P QPCR machine by following Sypro orange incorporation and the concurrent increase in fluorescence intensities at 570 nm.

ACCESSION NUMBERS

Cdk9/CycT/DRB and Cdk2/CycA/DRB coordinates have been deposited in the Protein Data Bank with accession codes 3MY1 and 3MY5, respectively.

SUPPLEMENTAL INFORMATION

Supplemental Information includes one figure and can be found with this article online at doi:10.1016/j.chembiol.2010.07.012.

ACKNOWLEDGMENTS

We thank the European Synchrotron Radiation Facility and staff for providing excellent facilities for data collection. We thank A. Echalier for the Cdk2/CycA proteins and A.J. Hole for helpful discussions. This work has been funded by the Medical Research Council.

Received: June 17, 2010
Revised: July 11, 2010
Accepted: July 12, 2010
Published: September 23, 2010

REFERENCES

Afonine, P.V., Gross-Kunstleve, R.W., and Adams, P.D. (2005). PHENIX REFINE. CCP4 News *42*, Contribution 8.

Auffinger, P., Hays, F.A., Westhof, E., and Ho, P.S. (2004). Halogen bonds in biological molecules. Proc. Natl. Acad. Sci. USA *101*, 16789–16794.

Battistutta, R., Mazzorana, M., Sarno, S., Kazimierczuk, Z., Zanotti, G., and Pinna, L.A. (2005). Inspecting the structure-activity relationship of protein kinase CK2 inhibitors derived from tetrabromo-benzimidazole. Chem. Biol. *12*, 1211–1219.

Baumli, S., Lolli, G., Lowe, E.D., Troiani, S., Rusconi, L., Bullock, A.N., Debreczeni, J.E., Knapp, S., and Johnson, L.N. (2008). The structure of P-TEFb (Cdk9/cyclin T1), its complex with flavopiridol and regulation by phosphorylation. EMBO J. *27*, 1907–1918.

Brown, N.R., Noble, M.E., Endicott, J.A., and Johnson, L.N. (1999). The structural basis for specificity of substrate and recruitment peptides for cyclin-dependent kinases. Nat. Cell Biol. *1*, 438–443.

Byrd, J.C., Lin, T.S., Dalton, J.T., Wu, D., Phelps, M.A., Fischer, B., Moran, M., Blum, K.A., Rovin, B., Brooker-McEldowney, M., et al. (2007). Flavopiridol administered using a pharmacologically derived schedule is associated with marked clinical efficacy in refractory, genetically high-risk chronic lymphocytic leukemia. Blood *109*, 399–404.

CCP4 (Collaborative Computational Project, Number 4). (1994). The CCP4 Suite: programs for protein crystallography. Acta Crystallogr. D Biol. Crystallogr. *50*, 760–763.

Core, L.J., and Lis, J.T. (2008). Transcription regulation through promoter-proximal pausing of RNA polymerase II. Science *319*, 1791–1792.

De Moliner, E., Brown, N.R., and Johnson, L.N. (2003). Alternative binding modes of an inhibitor to two different kinases. Eur J Biochem. *270*, 3174–3181.

Emsley, P., and Cowtan, K. (2004). Coot: model-building tools for molecular graphics. Acta Crystallogr. D Biol. Crystallogr. *60*, 2126–2132.

Lam, L.T., Pickeral, O.K., Peng, A.C., Rosenwald, A., Hurt, E.M., Giltnane, J.M., Averett, L.M., Zhao, H., Davis, R.E., Sathyamoorthy, M., et al. (2001). Genomic-scale measurement of mRNA turnover and the mechanisms of action of the anti-cancer drug flavopiridol. Genome Biol. *2*, RESEARCH0041.

Lommerse, J.P.M., Stone, A.J., Taylor, R., and Allen, F.H. (1996). The nature and geometry of intermolecular interactions between halogens and oxygen or nitrogen. J. Am. Chem. Soc. *118*, 3108–3116.

Lu, Y., Shi, T., Wang, Y., Yang, H., Yan, X., Luo, X., Jiang, H., and Zhu, W. (2009a). Halogen bonding–a novel interaction for rational drug design? J. Med. Chem. *52*, 2854–2862.

Lu, Y., Wang, Y., Xu, Z., Yan, X., Luo, X., Jiang, J., and Zhu, W. (2009b). C-X—H contacts in biomolecular systems: how they contribute to protein ligand binding affinity. J. Phys. Chem. B *113*, 12615–12621.

McCoy, A.J., Grosse-Kunstleve, R.W., Adams, P.D., Winn, M.D., Storoni, L.C., and Read, R.J. (2007). Phaser crystallographic software. J Appl Crystallogr. *40*, 658–674.

Peng, J., Marshall, N.F., and Price, D.H. (1998). Identification of a cyclin subunit required for the function of Drosophila P-TEFb. J. Biol. Chem. *273*, 13855–13860.

Peterlin, B.M., and Price, D.H. (2006). Controlling the elongation phase of transcription with P-TEFb. Mol. Cell *23*, 297–305.

Raaf, J., Brunstein, E., Issinger, O.G., and Niefind, K. (2008). The CK2 alpha/CK2 beta interface of human protein kinase CK2 harbors a binding pocket for small molecules. Chem. Biol. *15*, 111–117.

Sehgal, P.B., Darnell, J.E., Jr., and Tamm, I. (1976). The inhibition by DRB (5,6-dichloro-1-beta-D-ribofuranosylbenzimidazole) of hnRNA and mRNA production in HeLa cells. Cell *9*, 473–480.

Wang, S., and Fischer, P.M. (2008). Cyclin-dependent kinase 9: a key transcriptional regulator and potential drug target in oncology, virology and cardiology. Trends Pharmacol. Sci. *29*, 302–313.

Yamada, T., Yamaguchi, Y., Inukai, N., Okamoto, S., Mura, T., and Handa, H. (2006). P-TEFb-mediated phosphorylation of hSpt5 C-terminal repeats is critical for processive transcription elongation. Mol. Cell *21*, 227–237.

